

# Study of Robust Features in Formulating Guidance for Heuristic Algorithms for Solving the Vehicle Routing Problem

Bachtiar Herdianto<sup>1</sup>, Romain Billot<sup>1</sup>, Flavien Lucas<sup>2</sup>, and Marc Sevaux<sup>3</sup>

<sup>1</sup>*IMT Atlantique, Lab-STICC (UMR 6285, CNRS), Brest, France*

<sup>2</sup>*IMT Nord Europe, CERI Systèmes Numériques, Douai, France*

<sup>3</sup>*Université Bretagne Sud, Lab-STICC (UMR 6285, CNRS), Lorient, France*

[bachtiar.herdianto@imt-atlantique.fr](mailto:bachtiar.herdianto@imt-atlantique.fr)<sup>\*1</sup>

[romain.billot@imt-atlantique.fr](mailto:romain.billot@imt-atlantique.fr)<sup>1</sup>

[flavien.lucas@imt-nord-europe.fr](mailto:flavien.lucas@imt-nord-europe.fr)<sup>2</sup>

[marc.sevaux@univ-ubs.fr](mailto:marc.sevaux@univ-ubs.fr)<sup>3</sup>

## Abstract

The Vehicle Routing Problem (VRP) is a complex optimization problem with numerous real-world applications, mostly solved using metaheuristic algorithms due to its  $\mathcal{NP}$ -Hard nature. Traditionally, these metaheuristics rely on human-crafted designs developed through empirical studies. However, recent research shows that machine learning methods can be used to exploit the structural characteristics of solutions in combinatorial optimization, thereby aiding in designing more efficient algorithms, particularly for solving VRP. Building on this advancement, this study extends the previous research by conducting a sensitivity analysis using multiple classifier models that are capable of predicting the quality of VRP solutions. Hence, by leveraging explainable AI, this research is able to extend the understanding of how these models make decisions. Finally, our findings indicate that while feature importance varies, certain features consistently emerge as strong predictors. Furthermore, we propose a unified framework able to rank feature impact across different scenarios to illustrate this finding. These insights highlight the potential of feature importance analysis as a foundation for developing a guidance mechanism of metaheuristic algorithms for solving the VRP.

**Keywords**— Metaheuristic, Vehicle Routing Problem, Binary Classification, Explainable AI (XAI)

## 1 Introduction

Combinatorial optimization problems, such as Vehicle Routing Problems (VRP), are important in real-world applications as they search for efficient solutions to minimize costs.

Despite extensive research over decades, achieving optimal solutions remains a challenge (Laporte, 2009). Furthermore, the unique constraints of various problem variants demand specialized algorithms. The development of these algorithms is complex, making Machine Learning (ML) an attractive approach to improving the existing algorithms. Routing algorithms are typically divided into two categories: exact algorithms that offer global optimum but require many computational resources and heuristics methods for practical, real-world applications that mostly find a near-optimal solution. While most heuristics rely on human-designed strategies (Lucas et al., 2020), ML offers a new approach to improving algorithms. Moreover, the selection of features influenced by these ML models plays a critical role in effectively enhancing heuristic performances (Arnold and Sörensen, 2019b; Arnold and Sörensen, 2019a; Lucas, Billot, and Sevaux, 2019). Understanding the predictions of an ML model can be as crucial as the accuracy of the prediction itself in many applications (Lundberg and Lee, 2017).

The necessity to interpret predictions from tree models is more common (Lundberg et al., 2020), and explaining a series of models is fundamental for debugging the algorithm design (Chen, Lundberg, and Lee, 2022). Recent research on interpreting ML models has focused on feature attribution strategies. These methods assign a value to each input feature, indicating its importance in making a specific prediction. Feature attributions based on the Shapley value have gained favor for interpreting ML models (Chen et al., 2023; Liu and Barnard, 2023; Zern, Broelemann, and Kasneci, 2023). The integration of ML and optimization algorithms can be classified into three mechanisms: (1) end-to-end learning, (2) learning based on problem properties, and (3) learning repeated decisions (Bengio, Lodi, and Prouvost, 2021). Several studies demonstrate that learning based on problem properties and repeated decision-making is more favorable for solving larger and more realistic problems (Arnold and Sörensen, 2019a; Li, Yan, and Wu, 2021; Xin et al., 2021; Morabit, Desaulniers, and Lodi, 2021; Ma, Cao, and Chee, 2023; Morabit, Desaulniers, and Lodi, 2023). However, the features used in designing the learning method affect the performance of the developed hybrid algorithm.

This work builds upon previous contributions that focused on understanding the characteristics and features of high-quality VRP solutions (Arnold and Sörensen, 2019b; Lucas, Billot, and Sevaux, 2019). In this research, we conduct a sensitivity analysis of feature importance that influences a prediction model used to evaluate VRP solution quality. The primary objective is to analyze the behavior of problem features concerning solution quality across different scenarios. Prior work has shown that understanding the structural characteristics of solutions in combinatorial optimization helps design efficient algorithms, particularly for solving the VRP (Arnold and Sörensen, 2019b; Arnold and Sörensen, 2019a; Arnold, Gendreau, and Sörensen, 2019; Holanda Maia, Plastino, and Penna, 2020; Holanda Maia et al., 2022; Holanda Maia, Plastino, and Santos Souza, 2024; Mesa et al., 2025; Cavalcanti Costa, Mei, and Zhang, 2023; Santana, Lodi, and Vidal, 2023). While earlier studies laid the groundwork for understanding the importance of features in analyzing VRP solution quality (Arnold and Sörensen, 2019b; Lucas, Billot, and Sevaux, 2019), this study extends prior findings by incorporating multi-scenario and sensitivity analyses to uncover consistent and variable predictors of solution quality across diverse conditions.

The introduction of a mechanism for ranking feature importance further differentiates this work, providing additional insight for guiding the design of metaheuristic algorithms. Our goal is to identify a set of features with high potential for formulating guidelines to enhance metaheuristic algorithms, particularly for VRP. By uncovering these important characteristic solutions, we aim to provide a foundation for developing guidance able of improving the performance and effectiveness of metaheuristic algorithms in solving VRP.

## 1.1 Research Questions and Contributions

Due to the  $\mathcal{NP}$ -Hard nature of VRP, metaheuristic methods are often used to derive solutions as they provide high-quality results within a feasible time, especially for large and complex instances (Prodhon and Prins, 2016). Defining optimal solution properties has been found to benefit the design of efficient algorithms (Arnold and Sörensen, 2019a). Explainable learning models can transform VRP solving methods (Lucas, Billot, and Sevaux, 2019), potentially substituting human-crafted strategies. Machine learning model develop predictors that map data features to classes (Guidotti et al., 2018). By explaining these predictors, we understand feature utilization and integrate characteristic importance into rules for better guidance. In summary, this research addresses the following key questions:

1. What is the impact of each feature on the prediction accuracy of the VRP solution quality?
2. How does the feature importance vary across different scenarios?
3. Are there any features consistently strong predictors of solution quality regardless of the scenario?

In response to these questions, a comprehensive dataset of multi-scenario VRP solutions was generated to facilitate the development of a robust learning model applicable to different scenarios. Subsequently, a multi-scenario learning model was designed to examine the behavior of the features of VRP within these scenarios. A sensitivity analysis was then performed to explore each feature’s impact on the prediction model’s performance. Through this analysis, we identified features that consistently influenced the predictions of the developed learning model

across various scenarios. Additionally, to illustrate our findings, we proposed a novel formula to determine the order of feature importance, considering prediction accuracy across different scenarios. In summary, the main contributions of this research are:

1. A new dataset of multi-scenario VRP solutions for developing a robust learning model.
2. A robust multi-scenario learning model that assesses the behavior of VRP features.
3. A sensitivity analysis to determine each feature’s impact on the prediction model’s performance, as well as the variation and consistency of feature importance across the scenarios.
4. Introducing a novel formula to identify the order feature importance that considers prediction accuracy across different scenarios.

In the sequel, the paper is structured as follows: Section 2 details our approach for analyzing VRP features, Section 3 discusses feature behaviors and analyzes the findings, and Section 4 presents a unified explanation applicable across multiple scenarios.

## 2 Research Methodology

Our methodology to conduct a sensitivity analysis of feature importance is composed of four major steps: (1) generate data, (2) build a binary classification model across multi-scenario (defined in Definition 2.1), (3) explain the model using SHAP values, and (4) formulate a unified explanation formula, as shown in Figure 1. As the VRP is a complex problem with a wide variety of instances, we focus on the basic variant of VRP, which is the Capacitated Vehicle Routing Problem (CVRP). The CVRP can be characterized by an undirected graph  $G = (V, E)$ . The set of nodes  $V$  is composed of a depot  $c_0$  and a collection of customer nodes  $C$ , where  $C = \{c_1, c_2, \dots, c_V\}$  and  $\mathcal{V} = |V| - 1$  (Prodhon and Prins, 2016).

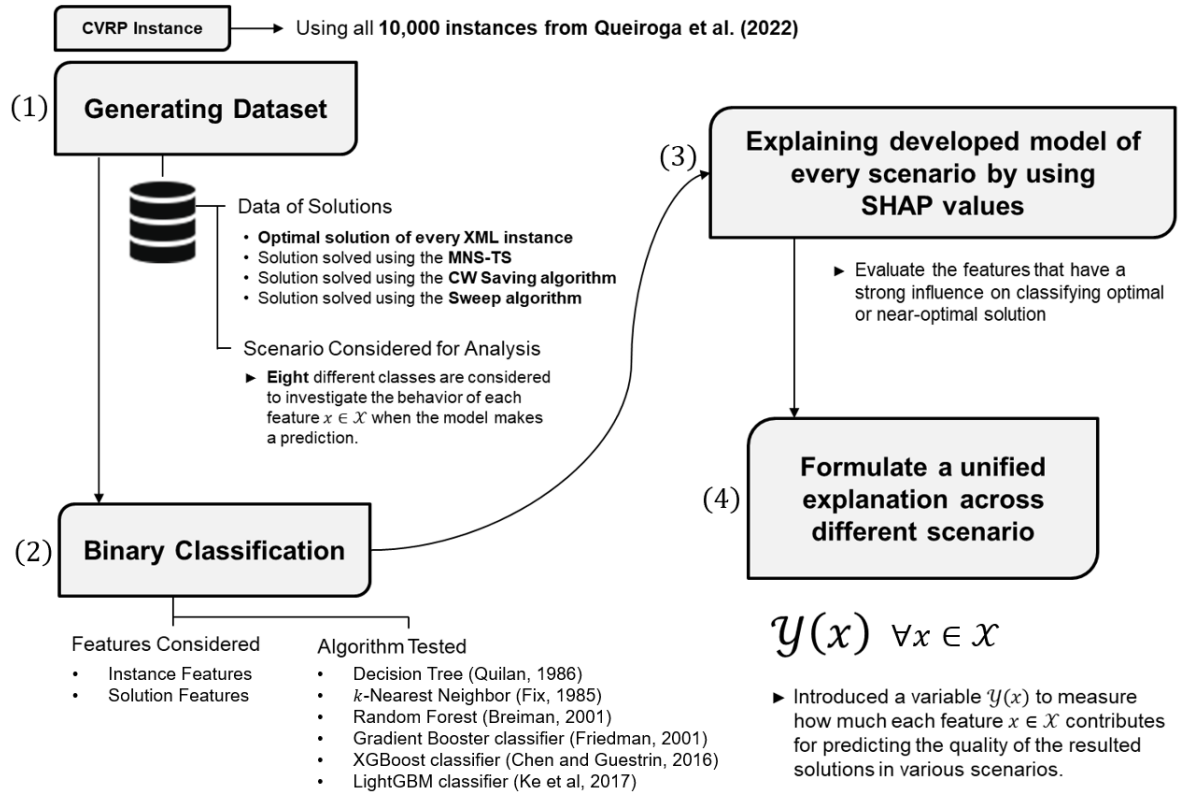


Figure 1: Research methodology used for sensitivity analysis of VRP’s feature importance.

**Definition 2.1** (Scenario). *A scenario refers to a specific configuration of data within a classification model, particularly focusing on the distribution of the positive ( $y_i = 1$ ) and negative ( $y_i = 0$ ) classes. In this context, the positive class represents optimal solutions, while the negative class consists of near-optimal solutions with a positive gap.*

In this research, the objective of the learning model  $\hat{f}$  is to classify between optimal and near-optimal solutions by performing a binary classification. Given a dataset  $\mathcal{D} = \{(\mathbf{x}_i, y_i)\}_{i=1}^N$ , where  $\mathbf{x}_i \in \mathbb{R}^d$  represents the feature vector for the  $i$ -th instance, and  $y_i \in \{0, 1\}$  is the corresponding binary label, the classifier  $\hat{f}$  can be represented as  $\hat{f} : \mathcal{X} \rightarrow \{0, 1\}$ , where  $\mathcal{X} = \mathbb{R}^d$  is the instance space and the  $d$  denotes the number of features. The  $N$  represents the total number of solution in the dataset  $\mathcal{D}$ , where each  $\mathbf{x}_i$  being a  $d$ -dimensional feature vector. The features  $d$  used in developing the learning model are described in Section 2.3.

## 2.1 Problem Instances Used and Optimal Solutions

The XML100 instances<sup>1</sup> are employed to generate solution data, which is subsequently used for analysis to comprehend feature behaviour and develop classification model  $f(\mathbf{x})$ . The 10,000 XML100 instances consist of a similar number of customer nodes, totalling 100 nodes each. However, they vary across different categories, such as the position of their depots, the distribution of customers, the distribution of demands, and the average size of the routes in their optimal solutions (Queiroga et al., 2021).

## 2.2 Data of Near-Optimal Solutions

To achieve binary classification between optimal solutions and near-optimal solutions using the model  $\hat{f}$ , we utilized the optimal solutions from every instance of the XML100 instances. To generate near-optimal solutions, we employed the MNS-TS algorithm (Soto et al., 2017; Lucas et al., 2020), the Clarke-Wright Savings algorithm (Clarke and Wright, 1964), and the Sweep algorithm (Gillett and Miller, 1974) on all XML100 instances<sup>2</sup>. The MNS-TS algorithm, which stands for *Multiple Neighborhood Search with Tabu Search*, has proven effective in solving both the Open VRP (OVRP) (Soto et al., 2017) and large-scale CVRP (Lucas et al., 2020).

**Definition 2.2** (Gap to Optimal). *Given  $Obj(\mathcal{Z}_1)$  as the total distance of optimal solution and  $Obj(\mathcal{Z}_0)$  as the total distance of near-optimal solution, the relative difference between the objective value of a near-optimal solution, as well as the value of the optimal solution are expressed as the gap to optimal, calculated as:*

$$\text{Gap to Optimal} := \frac{Obj(\mathcal{Z}_0) - Obj(\mathcal{Z}_1)}{Obj(\mathcal{Z}_1)} \times 100\% \quad (1)$$

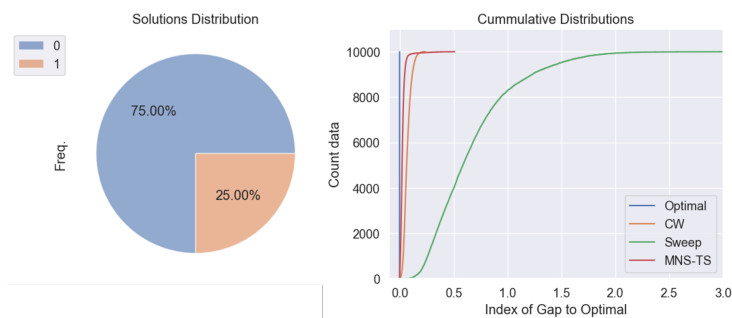


Figure 2: The pie chart (left) shows the dataset split into optimal ( $y_i = 1$ ) and near-optimal ( $y_i = 0$ ) solutions. The cumulative chart (right) shows the distribution of near-optimal solutions, where Sweep offers a wider range of solution qualities than the others.

<sup>1</sup>All the information related to the instances and their optimal solutions are available at <http://vrp.galgos.inf.puc-rio.br/index.php/en/>.

<sup>2</sup>The Clarke-Wright and Sweep algorithm were executed by using solver by Groër, Golden, and Wasil (2010), available at <https://github.com/coin-or/VRPH>.

Given Definition 2.1, for the analysis, the near-optimal solutions are divided into eight groups, each corresponding to a different scenario. These scenarios, along with their respective near-optimal solutions, are detailed in Table 1. These scenarios allow for the analysis of feature importance and model behavior under varying conditions of data distribution, particularly with respect to Definition 2.2.

Table 1: Detailed near-optimal solution for every scenario.

Scenario	Near-Optimal Solution Used for Analysis
Scenario 1: $S_1$	Solutions solved by the MNS-TS
Scenario 2: $S_2$	Solutions solved by the CW Saving algorithm
Scenario 3: $S_3$	Solutions solved by the Sweep algorithm
Scenario 4: $S_4$	All solutions with gap > 2%
Scenario 5: $S_5$	All solutions with gap > 5%
Scenario 6: $S_6$	All solutions with gap > 7%
Scenario 7: $S_7$	All solutions with gap > 10%
Scenario 8: $S_8$	All solutions with gap > 15%

Note: all scenarios include optimal solutions for comparison.

## 2.3 Features of Problem

This research categorizes the features for developing the learning model into instance-based and solution-based features. Some of these features are derived from the mean value or standard deviation (SD) of certain characteristics. The features used in this research are based on findings from prior recent studies (Herdianto et al., 2024). The instance-based and solution-based features are summarized in Table 2. In total, there are 9 features related to the instance characteristics and 22 features related to the characteristics of the resulting solution.

Table 2: Complete list of features used for analysis.

Instance-based Features	Solution-based Features	
<b>I01:</b> Number of customers	<b>S01:</b> Mean width of each route	<b>S12:</b> Mean terminal demand customer
<b>I02:</b> Number of vehicles	<b>S02:</b> SD the width of each route	<b>S13:</b> Mean the farthest customer’s demand
<b>I03:</b> Degree of capacity utilization	<b>S03:</b> Mean span of each route	<b>S14:</b> SD the farthest customer’s demand
<b>I04:</b> Mean customer-paired edge	<b>S04:</b> SD the span of each route	<b>S15:</b> SD the length of each route
<b>I05:</b> SD customer-paired edge	<b>S05:</b> Mean depth of each route	<b>S16:</b> Mean route-centroid distances
<b>I06:</b> Mean customer-depot edge	<b>S06:</b> SD the depth of each route	<b>S17:</b> SD route-centroid distances
<b>I07:</b> SD the customer-depot edge	<b>S07:</b> Route-edge ratio	<b>S18:</b> Mean degree of neighborhood
<b>I08:</b> Mean angular deviation of customers	<b>S08:</b> Mean max edge	<b>S19:</b> Mean route’s capacity utilization
<b>I09:</b> SD angular deviation of customers	<b>S09:</b> Longest-edge ratio	<b>S20:</b> SD route’s capacity utilization
	<b>S10:</b> longest-edge ratio	<b>S21:</b> Mean of longest distance-relatedness
	<b>S11:</b> Mean terminal edge	<b>S22:</b> SD of longest distance-relatedness

## 2.4 Classifier Baselines

For analyzing the behavior of features when predicting solutions, we developed the classifier model  $\hat{f}$  using several baseline classifiers, including  $k$ -Nearest Neighbors ( $k$ NN) (Fix, 1985), Decision Tree classifier (Quinlan, 1986), and Random Forest (Breiman, 2001).  $k$ NN is a simple, non-parametric classifier that classifies a data point based on the majority class of its  $k$ -nearest neighbors. Meanwhile, the Decision Tree classifier recursively splits the feature space to form a tree structure, making it easy to interpret but prone to overfitting. Random Forest addressed the mechanism of decision trees by combining multiple trees trained on random subsets of data and features. We also utilized various boosting algorithms, such as Gradient Boosting (Friedman, 2001), Extreme Gradient Boosting (XGBoost) (Chen and Guestrin, 2016), and Light Gradient Boosting Machine (LightGBM) (Ke et al., 2017).

Gradient Boosting is an ensemble method that builds decision trees sequentially, with each tree correcting the errors of the previous ones by optimizing a loss function. XGBoost refines the boosting mechanism by incorporating grow trees level-wise approach to reduce overfitting. LightGBM further refines this by using a histogram-based approach to find splits and grow trees leaf-wise (as opposed to XGBoost’s level-wise approach).

## 2.5 Metric Evaluation

The evaluation of the classifier  $\hat{f}$  is based on the confusion matrix. As outlined by (Narasimhan, Vaish, and Agarwal, 2014), the confusion matrix provides a tabular summary of the classification performance for a given dataset  $\mathcal{D}$ , comprises True Positives (TP), False Positives (FP), True Negatives (TN), and False Negatives (FN). The confusion matrix  $\mathcal{C}$  can be represent as a 2-dimensional matrix, as:

$$\mathcal{C} := \begin{bmatrix} \text{TN} & \text{FP} \\ \text{FN} & \text{TP} \end{bmatrix} \quad (2)$$

Given a threshold of 0.5 for the classifier  $\hat{f}$ , the classification rule is defined as follows: if  $\eta(\mathbf{x}) < 0.5$ , the prediction is  $\hat{f}(\mathbf{x}) = 0$  (considered a near-optimal solution), and if  $\eta(\mathbf{x}) \geq 0.5$ , the prediction is  $\hat{f}(\mathbf{x}) = 1$  (considered an optimal solution). Accordingly, the key components of  $\mathcal{C}$  in Equation (2) can be defined: TP as  $\text{TP} := \mathbb{P}(\hat{f}(\mathbf{x}) = 1 \wedge y = 1)$ , and TN as  $\text{TN} := \mathbb{P}(\hat{f}(\mathbf{x}) = 0 \wedge y = 0)$ . Similarly, FP is defined as  $\text{FP} := \mathbb{P}(\hat{f}(\mathbf{x}) = 1 \wedge y = 0)$ , and FN as  $\text{FN} := \mathbb{P}(\hat{f}(\mathbf{x}) = 0 \wedge y = 1)$ . Various metrics can be derived from the confusion matrix  $\mathcal{C}$  to evaluate the performance of  $\hat{f}$ , one of which is the Precision-Recall (PR) curve (Davis and Goadrich, 2006).

$$\text{recall} = \mathbb{P}(\hat{f}(\mathbf{x}) = 1 | y = 1) = \frac{\mathbb{P}(\hat{f}(\mathbf{x}) = 1 \wedge y = 1)}{\mathbb{P}(y = 1)} = \frac{\text{TP}}{\text{TP} + \text{FN}} \quad (3)$$

$$\text{precision} = \mathbb{P}(y = 1 | \hat{f}(\mathbf{x}) = 1) = \frac{\mathbb{P}(\hat{f}(\mathbf{x}) = 1 \wedge y = 1)}{\mathbb{P}(\hat{f}(\mathbf{x}) = 1)} = \frac{\text{TP}}{\text{TP} + \text{FP}} \quad (4)$$

Given the confusion matrix Equation (2), precision measures the accuracy of positive predictions, indicating the proportion of instances classified as positive that are actually positive. Meanwhile recall measures the proportion of actual positives correctly identified by the classifier (Narasimhan, Vaish, and Agarwal, 2014). Thus,  $F_\beta$ -score is used for quantifying the trade-off between precision and recall (Sokolova and Lapalme, 2009). The  $F_\beta$ -score is advantageous for evaluating binary classifiers, in particular with imbalanced data, because it balances precision and recall. In cases where one class is much more common than the other, metrics like accuracy can be misleading, as a classifier might achieve high accuracy by simply predicting the majority class. The  $F_\beta$ -score solve this issue by considering both FP and FN, making it a better performance indicator on the minority class.

**Definition 2.3** ( $F_\beta$ -score). *The  $F_\beta$ -score is defined as weighted average of precision and recall, calculated as:*

$$F_\beta\text{-score} := \frac{(\beta^2 + 1) \cdot \text{precision} \cdot \text{recall}}{\beta^2 \cdot \text{precision} + \text{recall}} \quad (5)$$

where  $\beta$  is a variable that controls the importance of recall in the overall score.

Given Definition 2.3, by substituting  $\beta = 1$  into Equation (5), the  $F_\beta$ -score provides a balanced measure of precision and recall, known as the  $F_1$ -score. Thus, in this research will utilize the  $F_1$ -score as the key metric to evaluate the classifier’s performance in every scenario as it able for ensuring the classifier  $\hat{f}$  perform well with respect to the positive class  $y_i = 1$  (optimal solutions).

## 2.6 Model Interpretability

Model interpretability is the ability to interpret and understand how a machine learning model able to generates its predictions and decisions (Guidotti et al., 2018). Model interpretability can be achieved by providing understandable explanations for every predictions. Various methods exist to achieve model explainability, one of them is the SHAP value (Lundberg et al., 2017; 2020; Baptista et al., 2022). SHAP values quantify the contribution

of each feature by assessing the effect of its inclusion in every possible subset of the remaining features, thereby capturing feature interactions.

**Definition 2.4** (SHAP (SHapley Additive exPlanations)). *Let  $\phi_j$  represents the SHAP value for feature  $j$ , reflecting its average contribution to the model’s output across all possible feature combinations. Assume  $\mathbf{D}$  as the set of all features, where the  $d$  represents  $|\mathbf{D}|$ . Then, the  $\mathbf{U}$  is a subset of  $\mathbf{D}$  that does not include  $j$ , where the  $u$  represents the size of  $\mathbf{U}$ . Thus, assume  $v(\mathbf{U})$  is the value function, which typically represents the model’s prediction when only features in set  $\mathbf{U}$  are considered. For interpreting ML models, the SHAP value for feature  $j$  is computed by considering all possible subsets of features excluding  $j$  and the change in the prediction of the classifier when  $j$  is added to the subset. The SHAP value for feature  $j$  is given by:*

$$\phi_j := \sum_{\mathbf{U} \subseteq \mathbf{D} \setminus \{j\}} \frac{u!(d-u-1)!}{d!} [v(\mathbf{U} \cup \{j\}) - v(\mathbf{U})] \quad (6)$$

Hence, given by Definition 2.4, we can know that a higher absolute mean SHAP value of a feature indicates a stronger influence of that feature on the model’s predictions. Moreover, SHAP values also provide several advantages, including interaction awareness. SHAP values capture feature interactions by calculating each feature’s contribution to predictions, offering a comprehensive understanding of feature importance (Lundberg and Lee, 2017).

### 3 Data Mining Analysis

As summarized in Figure 1, several classifiers were performed on the dataset for each scenario. The best classifier was then further analyzed to obtain its SHAP values<sup>3</sup>, providing insights into the contribution and impact of each feature on the model’s predictions.



Figure 3: Performance of classifiers in every scenario.

In Figure 3, the performance of various classifiers across 8 scenarios is summarized. Meanwhile Figure 4 shows the global feature importance based on SHAP values of filtered features. In the first 3 scenarios, individual heuristic algorithms were used to generate solutions. Gradient Boosting and X-Gradient Boosting classifiers consistently achieved the highest  $F_1$ -scores, while  $k$ -NN lagged behind. Features like S19 and S18, representing the average rank of the neighborhood and capacity utilization of the VRP, respectively, were consistently identified as the most important across all scenarios, underscoring their important role in model prediction. In scenarios four

<sup>3</sup>The dataset, the source code and the documentation for performing the analysis can be found at <https://github.com/bachtiarherdianto/Modelling-XAI-CVRP>.

through eight, solutions from all 3 algorithms were combined, focusing on those with increasing gaps from the optimal solutions to be more diversified solutions. The performance of the classifiers generally improved as the quality solution diversified, a similar trend to the previous first 3 scenarios. This trend is further explained in Proposition 3.1. Meanwhile, in Figure 4, each scenario demonstrated unique distributions of feature significance, with some scenarios showing one or two dominant features while others exhibited a more balanced spread. For instance, Scenario 3 had a clear standout feature (S07), whereas in Scenario 5, the distribution of importance was more even among several features like I03, S11, and S18. These variations suggested the dynamic nature of feature importance across different models, datasets, or conditions, where feature significance could shift depending on the specific scenario.

**Proposition 3.1.** *Let  $Z_1^m$  represent the data points  $y_i = 1$  (optimal solutions) in scenario  $m \in M$ , and  $Z_0^m$  as  $y_i = 0$  (near-optimal solutions). If a dataset of a scenario  $m$  exhibits a wide variety in the distribution of data points such that the gap between  $Z_1^m$  and  $Z_0^m$  are diverse, then the classifier  $\hat{f}$  will perform better, as measured by the  $F_1$ -score.*

*Proof.* Given the formulation of gap to optimal in Equation (1) and  $F_1$ -score in Equation (5) when  $\beta = 1$ , we can conclude that with better separation and fewer miss-classifications between  $Z_1$  and  $Z_0$ , precision improves as  $\hat{f}$  has less FP. Moreover, a diverse dataset helps the classifier  $\hat{f}$  improves recall by reducing FN.  $\square$

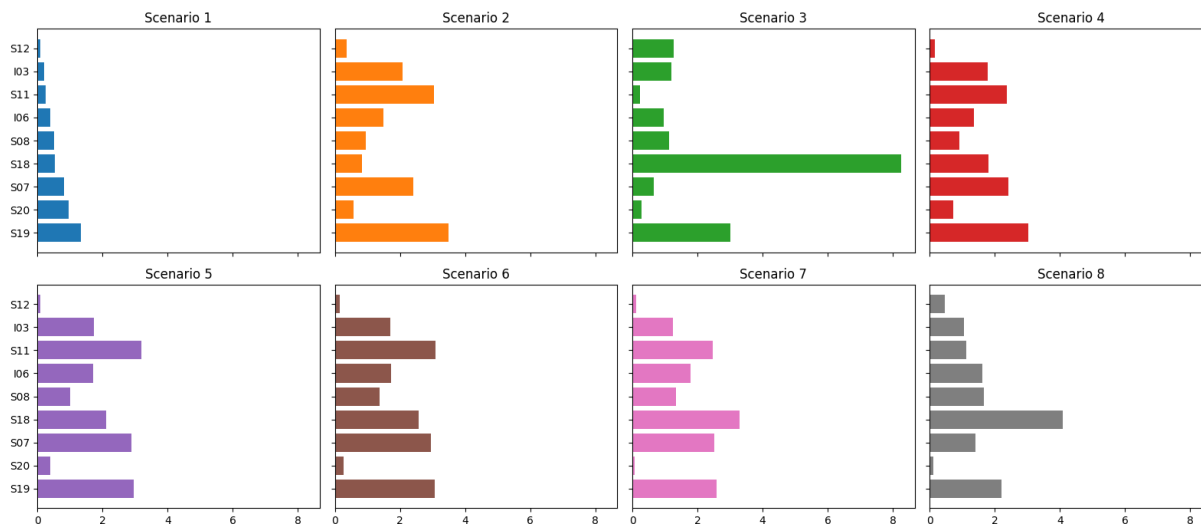


Figure 4: SHAP value of filtered features in every scenario.

Figure 5 illustrate the SHAP values of several strong features in three selected highest  $F_1$ -score scenarios. Across all selected scenarios, S18 and S19 repeatedly emerge as the most importance features. The color gradient in the plot represents the behavior of the features, where higher values of S19 (indicated by red points) are often associated with positive SHAP values, which correlate with better solution quality. Conversely, lower values of S18 (blue points) could also correspond to better solution quality, as indicated by their positive SHAP values. This suggests that while S18 and S19 are consistently important, their impact on solution quality can vary depending on whether their values are high or low. Moreover, given by Definition 2.1 and Equation (6), we can conclude that the directional impact of SHAP values for any given feature will mostly similar across different scenarios. However, the order of feature importance can vary between scenarios. This is because the direction of a feature’s SHAP value  $\phi_j$  is mostly preserved because the scalar relationship between the feature and the target variable mostly similar. Meanwhile, the absolute values can differ as the influences of features across scenarios vary, leading to the variation order of feature importance.

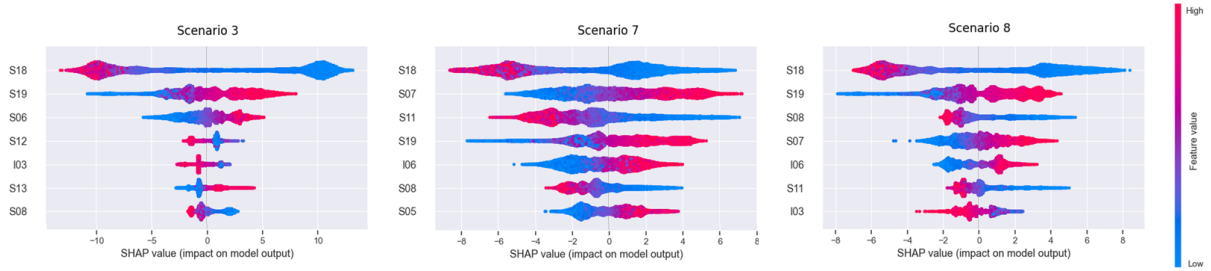


Figure 5: The local explanation summary plot for filtered features from selected scenarios.

A shows the details of the global feature importance plots and the local explanation summary plot for every scenario. The global feature importance plot can be used to identify which features are most important in the decision-making process, while the local explanation summary plot is useful for understanding the behaviour of features when the model makes a prediction.

## 4 Modelling Across Multi-Scenario

As shown in Figure 4 and 5, features S18 and S19 frequently emerge as the most important features in several scenarios. This happens particularly in scenario 3, indicating their significant contribution in characterizing solution quality. However, this dominance is only sometimes apparent, as shown in Figure 4. The other features, such as S11, S07, and I03, also exhibit significant influence in several other scenarios, making it seem that they might be equally influential. The apparent competitiveness of these other features can create the impression that S18 and S19 are not overwhelmingly strong influences  $\hat{f}$ . Nevertheless, when considering the  $F_1$ -score associated with each scenario, the actual effect of S18 and S19 becomes clearer. With factoring in the  $F_1$ -scores, the comparative strength of S18 and S19 might seem more convincing. Given this analysis, Definition 4.1 explain how to visualize in a simple manner the feature importance rank across different tested scenarios.

**Definition 4.1.** Given the SHAP value  $S^m(x)$  of a feature  $x$  in scenario  $m$  and the  $F_1$ -score $_m$  of the classifier in that scenario, the overall contribution  $\mathcal{Y}(x)$  of feature  $x$  to the quality of solutions across multiple scenarios is defined as:

$$\mathcal{Y}(x) = \sum_{m \in M} (S^m(x) \times F_1\text{-score}_m) \quad (7)$$

where  $M$  is the set of all scenarios, and  $S^m(x)$  is the mean of the absolute SHAP values of feature  $x$  in scenario  $m$ .

From Equation (7), we can see that the SHAP value  $S^m(x)$  quantifies the impact of a feature on model predictions in a given scenario  $m \in M$ , where  $M = 8$  (as summarized in Table 1). Meanwhile, The  $F_1$ -score shows the model's accuracy. To determine the overall contribution  $\mathcal{Y}(x)$  of a feature across all scenarios, we weight its SHAP values by the respective scenario's  $F_1$ -score and sum them across all scenarios. Given Definition 2.3 and 2.4, Equation (7) captures the cumulative influence of a feature by considering its impact on model's predictions and the model's performance.

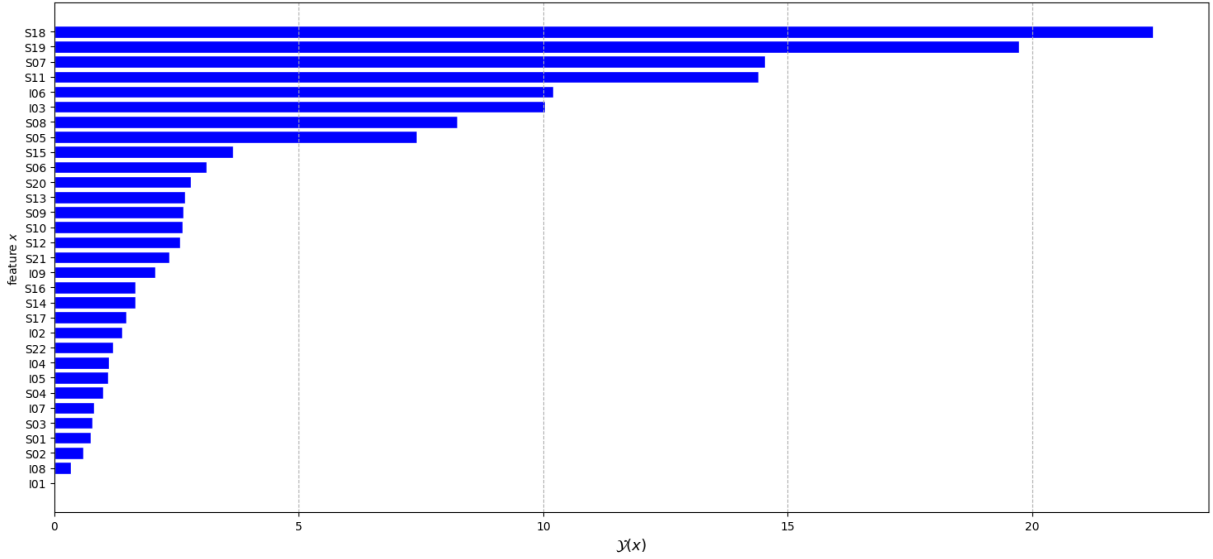


Figure 6: The representation of the VRP’s feature importance across multiple tested scenarios.

Figure 6 illustrates the relative importance of various features across multiple scenarios, recognizing S18 and S19 as the most significant. These features consistently contribute significantly to the model’s prediction. S07, S11, S11, I06, and I03 (summarized in Table 2) are also important but have a lower impact compared to the previous features. Meanwhile, features like S09, S10, S12, and S21 show lower importance, with I08 and I01 being the weakest across the scenarios. Then, from Figure 6, we can see that if a feature  $x$  has a very high SHAP value  $S^m(x)$  in a single scenario  $m \in M$ , and the scenario also has a relatively high  $F_1$ -score $_m$ , compared to other scenarios, then feature  $x$  will still maintain significant importance across different scenarios as reflected in its overall contribution  $\mathcal{Y}(x)$ . Meanwhile, from Figure 6, we also see that if a feature  $x$  consistently has high SHAP values  $S^m(x)$  across multiple scenarios where the  $F_1$ -score is also high, then  $\mathcal{Y}(x)$  will be significantly higher than other features. This implies that feature  $x$  is critically important to the model’s predictive performance across those scenarios.

This comprehensive understanding of feature importance provides a clearer direction of how the feature behaves when deciding. The analysis highlights the significance of S18 and S19 as key predictors, underlines the consistent influence of S19 and S18 on model predictions across different scenarios. Unlike prior studies that emphasized average route width as the main characteristic (Arnold and Sørensen, 2019b; Lucas, Billot, and Sevaux, 2019), our analysis across multiple scenarios identified a new and more robust characteristic for indicating solution quality. Subsequently, since  $F_1$ -score is a positive scalar, given  $\mathcal{Y}(x)$  from Equation (7), the SHAP’s directional behavior of a feature’s influence on classifier model predictions is preserved. This because from Equation (6), when multiplying the SHAP value  $\phi(x)$  of a feature  $x$  in a scenario  $m$  by a scalar value  $F_1$ -score $_m$ , the direction of  $\phi(x)$  does not change. Based on this fact, we can more precisely define the relationship between these features and solution quality. In particular, higher values of S19 consistently emerge as an indicators of better solution quality with lower gap (as described in Definition 2.2), suggesting that as S19 increases, the likelihood of achieving a lower gap of a solution. Conversely, lower values of S18 appear to correspond with improved solution quality, indicating that when S18 decreases, the model is more likely to generate a lower gap of a solution.

## 5 Conclusion

In this research, we investigated the influence and variability of individual features on predicting the solution quality of the Vehicle Routing Problem (VRP). We examined how each feature impacts model performance and how the importance of these features varies across different scenarios. By constructing a comprehensive dataset encompassing multiple scenarios, we developed a robust multi-scenario learning model capable of interpreting VRP feature behavior under varied conditions. Sensitivity analysis was employed to quantify each feature's impact, revealing several features that consistently influenced model performance. Additionally, we observed that a more diverse gap among near-optimal solutions enhances classification accuracy, as better separation leads to fewer false positives and reduced false negatives. To support our findings, we introduced a new formula for determining feature importance, incorporating prediction accuracy across scenarios. This work advances the understanding of feature behavior in predictive models and enhances the interpretability of VRP solution quality predictions beyond prior studies.

While this study provides valuable insights, it represents only a starting point toward developing feature-based guidance mechanisms. The derived rules offer the potential for more precise adjustments of methods and settings based on the specific needs of each situation within the heuristic process. This opens the possibility of developing a robust guidance mechanism within metaheuristic algorithms for solving the VRP.

# A Appendix: The Global Feature Importance (left) and Local Explanation Summary (right) Plots for Every Scenario

## A.1 Scenario 1

Table 3: Performance of several baseline classifier used in the scenario 1.

Algorithm	Precision	Recall	$F_1$ -score
K-Nearest Neighbors Classifier	0.476	0.351	0.404
Decision Tree Classifier	0.537	0.538	0.538
Random Forest Classifier	0.523	0.500	0.511
<b>Gradient Boosting Classifier</b>	<b>0.672</b>	<b>0.661</b>	<b>0.666</b>
X-Gradient Boosting Classifier	0.632	0.621	0.627
Light Gradient Boosting Classifier	0.652	0.652	0.652

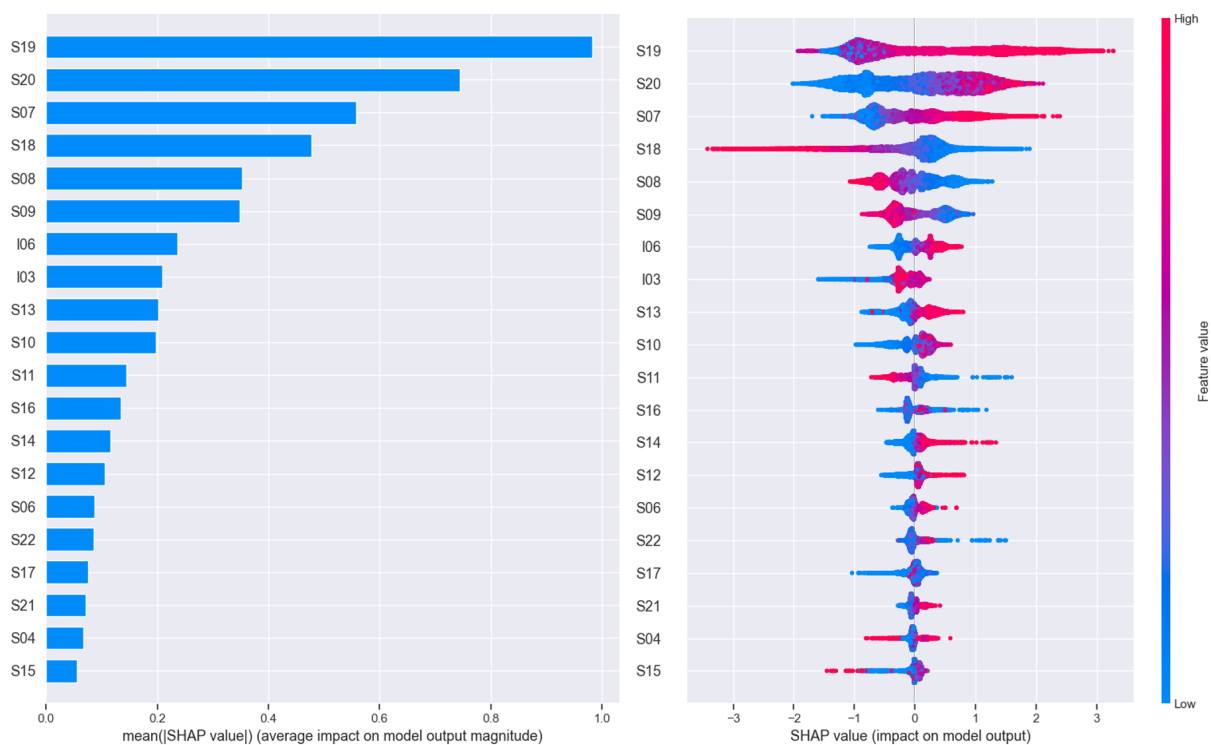


Figure 7: Plot of scenario 1 by using Gradient Boosting classifier with  $F_1$ -score = 0.666.

## A.2 Scenario 2

Table 4: Performance of several baseline classifier used in the scenario 2.

Algorithm	Precision	Recall	$F_1$ -score
K-Nearest Neighbors Classifier	0.609	0.483	0.539
Decision Tree Classifier	0.742	0.731	0.736
Random Forest Classifier	0.785	0.807	0.796
Gradient Boosting Classifier	0.860	0.905	0.882
<b>X-Gradient Boosting Classifier</b>	<b>0.870</b>	<b>0.907</b>	<b>0.888</b>
Light Gradient Boosting Classifier	0.854	0.900	0.876

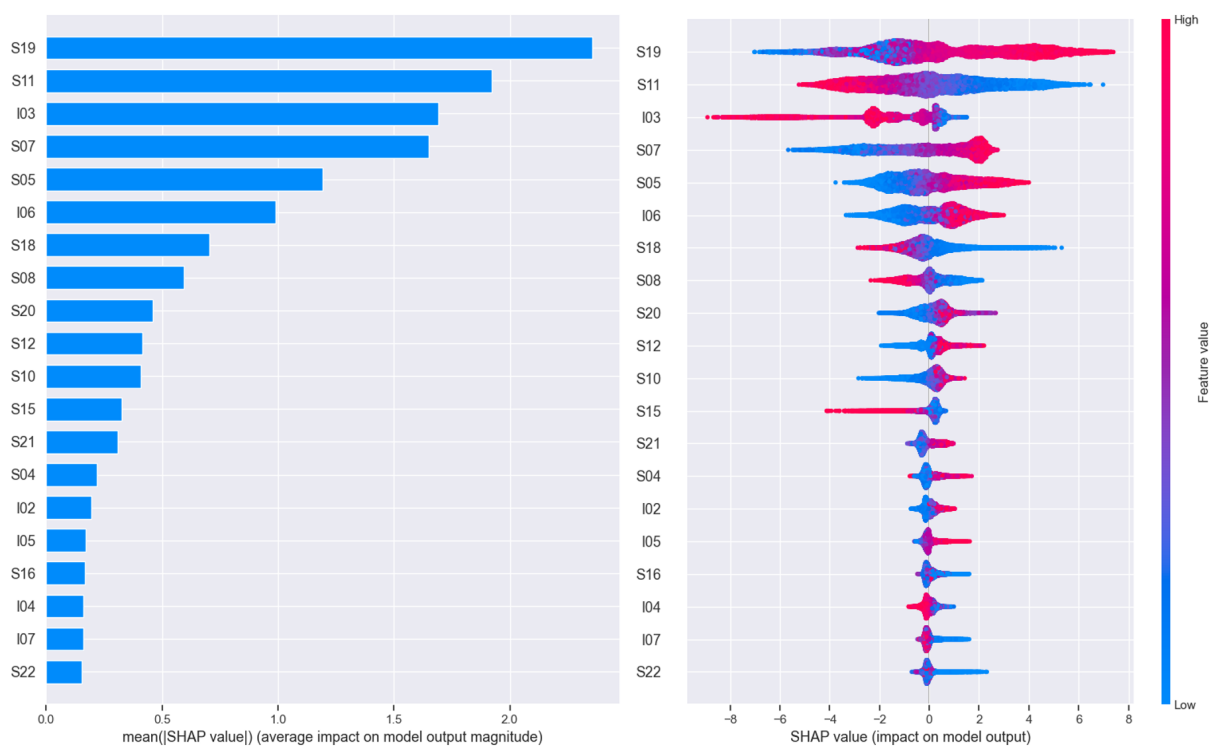


Figure 8: Plot of scenario 2 by using X-Gradient Boosting classifier with  $F_1$ -score = 0.888.

### A.3 Scenario 3

Table 5: Performance of several baseline classifier used in the scenario 3.

Algorithm	Precision	Recall	$F_1$ -score
K-Nearest Neighbors Classifier	0.913	0.891	0.902
Decision Tree Classifier	0.990	0.992	0.990
Random Forest Classifier	0.999	0.996	0.997
<b>Gradient Boosting Classifier</b>	<b>0.999</b>	<b>0.999</b>	<b>0.999</b>
X-Gradient Boosting Classifier	0.999	0.998	0.999
Light Gradient Boosting Classifier	0.998	0.998	0.998

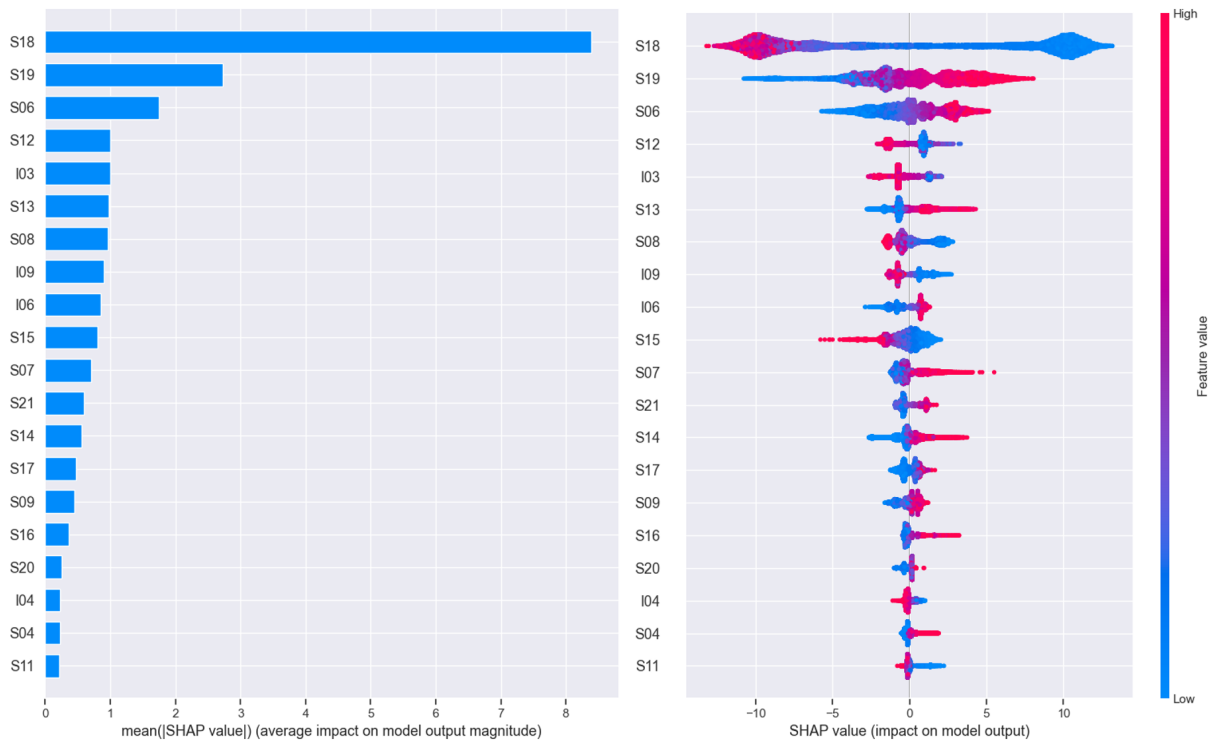


Figure 9: Plot of scenario 3 by using Gradient Boosting classifier with  $F_1$ -score = 0.999.

## A.4 Scenario 4

Table 6: Performance of several baseline classifier used in the scenario 4.

Algorithm	Precision	Recall	$F_1$ -score
K-Nearest Neighbors Classifier	0.430	0.647	0.517
Decision Tree Classifier	0.545	0.732	0.625
Random Forest Classifier	0.572	0.910	0.702
Gradient Boosting Classifier	0.676	0.907	0.775
<b>X-Gradient Boosting Classifier*</b>	<b>0.723</b>	<b>0.837</b>	<b>0.775</b>
Light Gradient Boosting Classifier	0.660	0.904	0.763

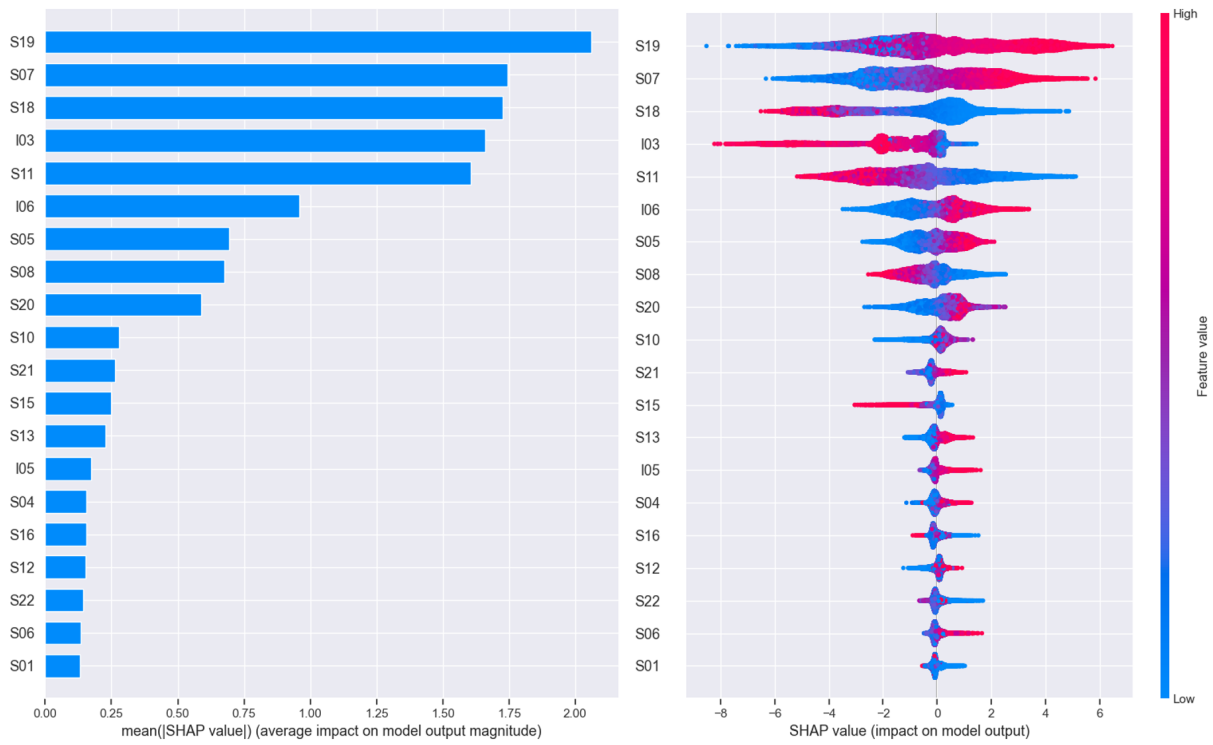


Figure 10: Plot of scenario 4 by using X-Gradient Boosting classifier with  $F_1$ -score = 0.775.

## A.5 Scenario 5

Table 7: Performance of several baseline classifier used in the scenario 5.

Algorithm	Precision	Recall	$F_1$ -score
K-Nearest Neighbors Classifier	0.620	0.769	0.686
Decision Tree Classifier	0.765	0.828	0.791
Random Forest Classifier	0.827	0.892	0.858
Gradient Boosting Classifier	0.863	0.963	0.910
<b>X-Gradient Boosting Classifier</b>	<b>0.895</b>	<b>0.951</b>	<b>0.922</b>
Light Gradient Boosting Classifier	0.856	0.961	0.906

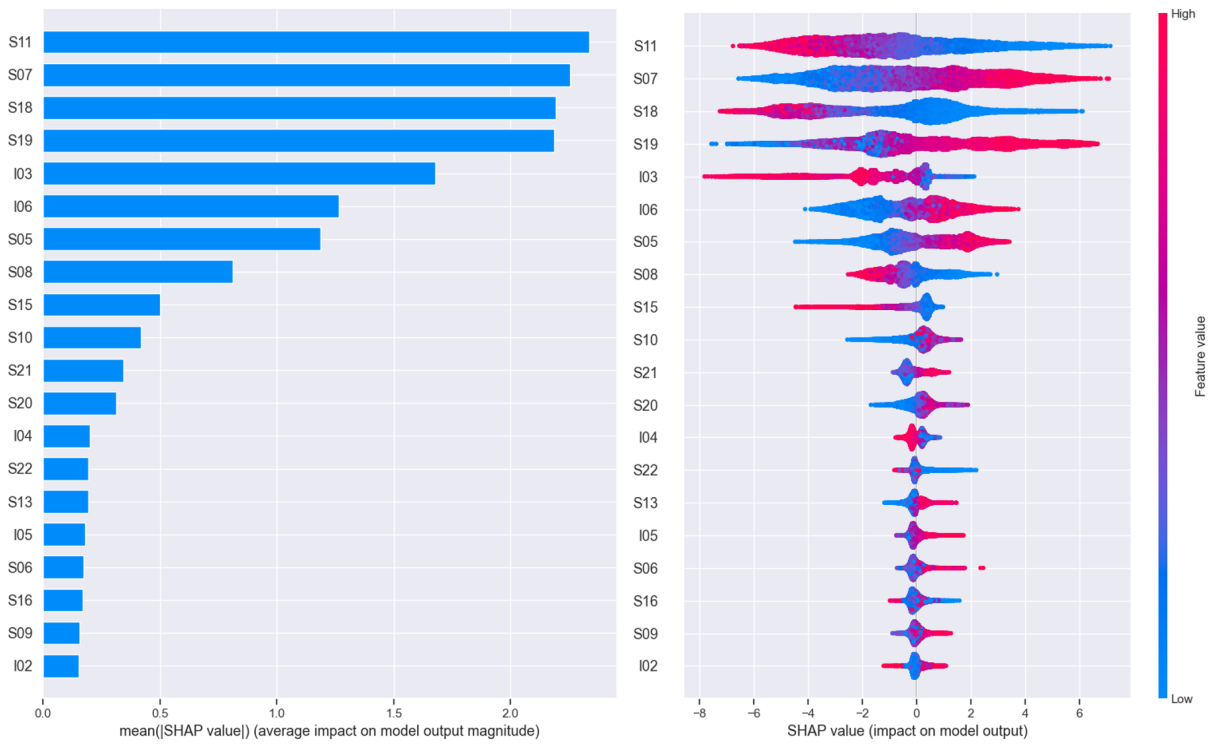


Figure 11: Plot of scenario 5 by using X-Gradient Boosting classifier with  $F_1$ -score = 0.922.

## A.6 Scenario 6

Table 8: Performance of several baseline classifier used in the scenario 6.

Algorithm	Precision	Recall	$F_1$ -score
K-Nearest Neighbors Classifier	0.720	0.824	0.768
Decision Tree Classifier	0.841	0.881	0.863
Random Forest Classifier	0.887	0.962	0.923
Gradient Boosting Classifier	0.924	0.979	0.951
<b>X-Gradient Boosting Classifier</b>	<b>0.941</b>	<b>0.978</b>	<b>0.959</b>
Light Gradient Boosting Classifier	0.924	0.981	0.952

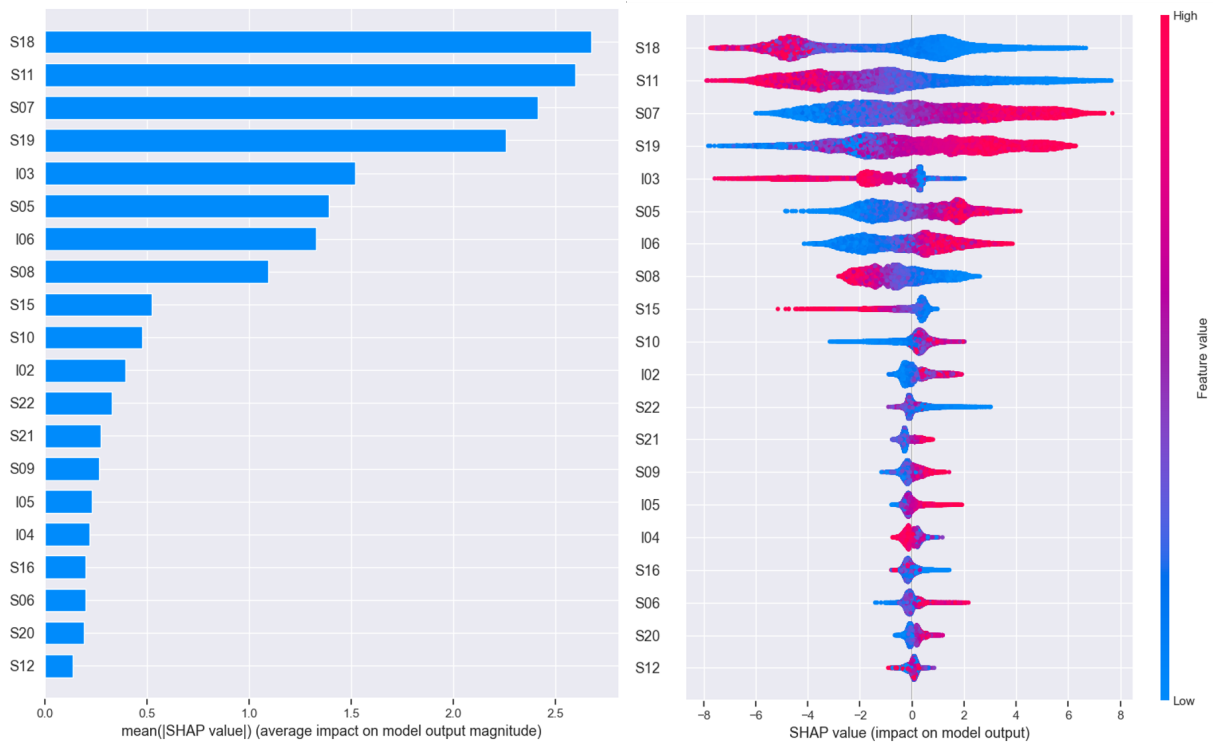


Figure 12: Plot of scenario 6 by using X-Gradient Boosting classifier with  $F_1$ -score = 0.959.

## A.7 Scenario 7

Table 9: Performance of several baseline classifier used in the scenario 7.

Algorithm	Precision	Recall	$F_1$ -score
K-Nearest Neighbors Classifier	0.827	0.871	0.848
Decision Tree Classifier	0.928	0.933	0.930
Random Forest Classifier	0.936	0.991	0.962
Gradient Boosting Classifier	0.966	0.991	0.979
<b>X-Gradient Boosting Classifier</b>	<b>0.972</b>	<b>0.994</b>	<b>0.983</b>
Light Gradient Boosting Classifier	0.967	0.994	0.980

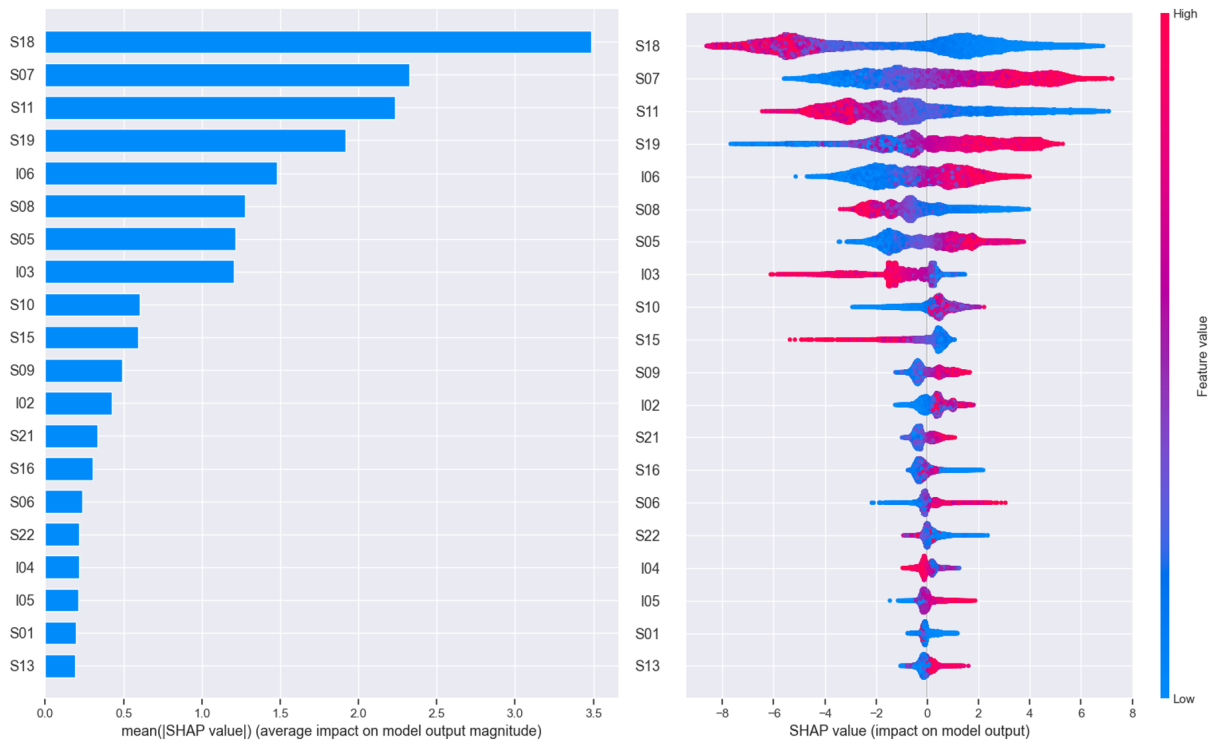


Figure 13: Plot of scenario 7 by using X-Gradient Boosting classifier with  $F_1$ -score = 0.983.

## A.8 Scenario 8

Table 10: Performance of several baseline classifier used in the scenario 8.

Algorithm	Precision	Recall	$F_1$ -score
K-Nearest Neighbors Classifier	0.895	0.896	0.895
Decision Tree Classifier	0.980	0.976	0.978
Random Forest Classifier	0.985	0.998	0.991
<b>Gradient Boosting Classifier*</b>	<b>0.993</b>	<b>0.999</b>	<b>0.996</b>
X-Gradient Boosting Classifier	0.992	0.998	0.996
Light Gradient Boosting Classifier	0.992	0.998	0.995

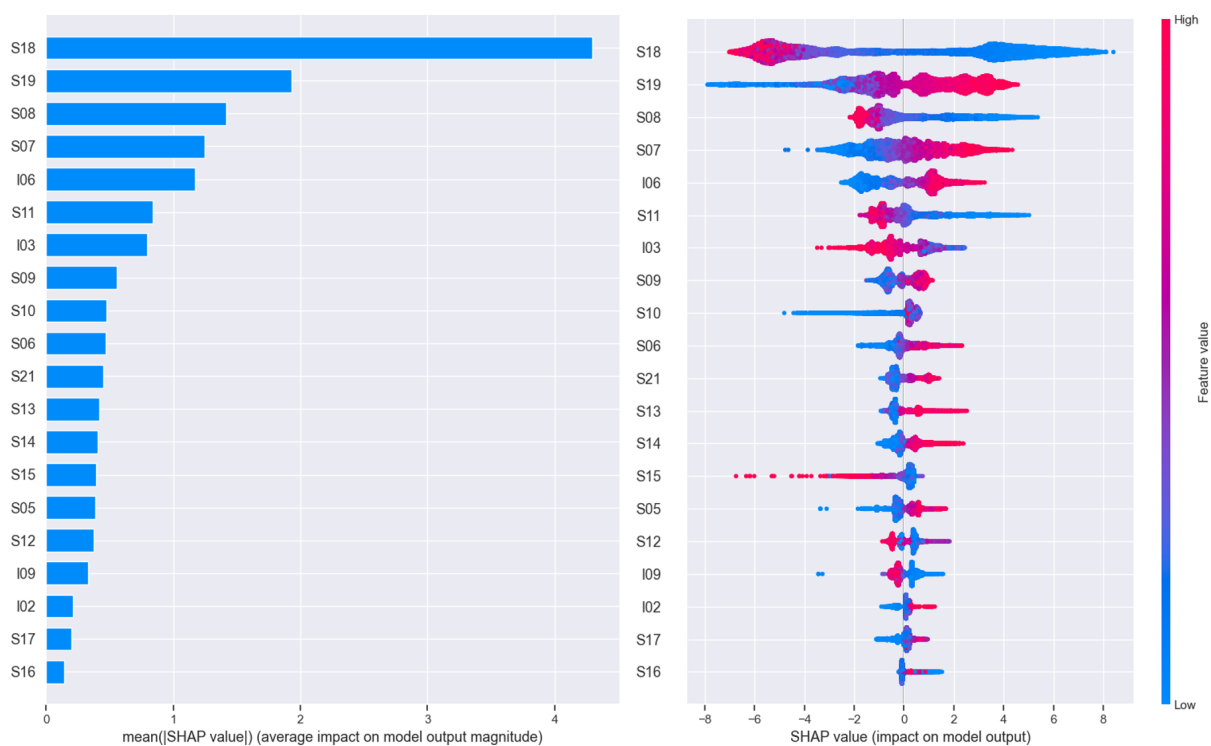


Figure 14: Plot of scenario 8 by using Gradient Boosting classifier with  $F_1$ -score = 0.996.

## References

- [1] Florian Arnold, Michel Gendreau, and Kenneth Sörensen. “Efficiently solving very large-scale routing problems”. In: *Computers & Operations Research* 107 (2019), pp. 32–42. ISSN: 0305-0548.
- [2] Florian Arnold and Kenneth Sörensen. “Knowledge-guided local search for the vehicle routing problem”. In: *Computers & Operations Research* 105 (2019), pp. 32–46.
- [3] Florian Arnold and Kenneth Sörensen. “What makes a VRP solution good? The generation of problem-specific knowledge for heuristics”. In: *Computers & Operations Research* 106 (2019), pp. 280–288.
- [4] Marcia L Baptista, Kai Goebel, and Elsa MP Henriques. “Relation between prognostics predictor evaluation metrics and local interpretability SHAP values”. In: *Artificial Intelligence* 306 (2022), p. 103667.
- [5] Yoshua Bengio, Andrea Lodi, and Antoine Prouvost. “Machine learning for combinatorial optimization: a methodological tour d’horizon”. In: *European Journal of Operational Research* 290.2 (2021), pp. 405–421.
- [6] Leo Breiman. “Random forests”. In: *Machine learning* 45 (2001), pp. 5–32.
- [7] Joao Guilherme Cavalcanti Costa, Yi Mei, and Mengjie Zhang. “Learning to select initialisation heuristic for vehicle routing problems”. In: *Proceedings of the Genetic and Evolutionary Computation Conference*. 2023, pp. 266–274.
- [8] Hugh Chen, Scott M Lundberg, and Su-In Lee. “Explaining a series of models by propagating Shapley values”. In: *Nature communications* 13.1 (2022), p. 4512.
- [9] Hugh Chen et al. “Algorithms to estimate Shapley value feature attributions”. In: *Nature Machine Intelligence* 5.6 (2023), pp. 590–601.
- [10] Tianqi Chen and Carlos Guestrin. “Xgboost: A scalable tree boosting system”. In: *Proceedings of the ACM SIGKDD Conference on Knowledge Discovery and Data Mining*. 2016, pp. 785–794.
- [11] Geoff Clarke and John W Wright. “Scheduling of vehicles from a central depot to a number of delivery points”. In: *Operations research* 12.4 (1964), pp. 568–581.
- [12] Jesse Davis and Mark Goadrich. “The relationship between Precision-Recall and ROC curves”. In: *Proceedings of the International Conference on Machine Learning*. 2006, pp. 233–240.
- [13] Evelyn Fix. *Discriminatory analysis: nonparametric discrimination, consistency properties*. Vol. 1. USAF school of Aviation Medicine, 1985.
- [14] Jerome H Friedman. “Greedy function approximation: a gradient boosting machine”. In: *Annals of statistics* (2001), pp. 1189–1232.
- [15] Billy E Gillett and Leland R Miller. “A heuristic algorithm for the vehicle-dispatch problem”. In: *Operations research* 22.2 (1974), pp. 340–349.
- [16] Chris Groër, Bruce Golden, and Edward Wasil. “A library of local search heuristics for the vehicle routing problem”. In: *Mathematical Programming Computation* 2 (2010), pp. 79–101.
- [17] Riccardo Guidotti et al. “A survey of methods for explaining black box models”. In: *ACM computing surveys (CSUR)* 51.5 (2018), pp. 1–42.
- [18] Bachtiar Herdianto et al. “Metaheuristic Enhanced with Feature-Based Guidance and Diversity Management for Solving the Capacitated Vehicle Routing Problem”. In: *arXiv preprint arXiv:2407.20777* (2024).

- [19] Marcelo Rodrigues de Holanda Maia, Alexandre Plastino, and Puca Huachi Vaz Penna. “MineReduce: An approach based on data mining for problem size reduction”. In: *Computers & Operations Research* 122 (2020), p. 104995.
- [20] Marcelo Rodrigues de Holanda Maia, Alexandre Plastino, and Uéverton dos Santos Souza. “An improved hybrid genetic search with data mining for the CVRP”. In: *Networks* 4.83 (2024), pp. 692–711.
- [21] Marcelo Rodrigues de Holanda Maia et al. “Interpretable ensembles of classifiers for uncertain data with bioinformatics applications”. In: *IEEE/ACM Transactions on Computational Biology and Bioinformatics* 20.3 (2022), pp. 1829–1841.
- [22] Guolin Ke et al. “Lightgbm: A highly efficient gradient boosting decision tree”. In: *Advances in neural information processing systems* 30 (2017).
- [23] Gilbert Laporte. “Fifty years of vehicle routing”. In: *Transportation science* 43.4 (2009), pp. 408–416.
- [24] Sirui Li, Zhongxia Yan, and Cathy Wu. “Learning to delegate for large-scale vehicle routing”. In: *Advances in Neural Information Processing Systems* 34 (2021), pp. 26198–26211.
- [25] Tommy Liu and Amanda S Barnard. “Shapley based residual decomposition for instance analysis”. In: *Proceedings of the International Conference on Machine Learning*. 2023, pp. 21375–21387.
- [26] Flavien Lucas, Romain Billot, and Marc Sevaux. “A comment on “what makes a VRP solution good? The generation of problem-specific knowledge for heuristics””. In: *Computers & Operations Research* 110 (2019), pp. 130–134.
- [27] Flavien Lucas et al. “Reducing space search in combinatorial optimization using machine learning tools”. In: *Learning and Intelligent Optimization: 14th International Conference, LION 14, Athens, Greece, May 24–28, 2020, Revised Selected Papers 14*. Springer. 2020, pp. 143–150.
- [28] Scott M Lundberg and Su-In Lee. “A unified approach to interpreting model predictions”. In: *Advances in neural information processing systems* 30 (2017).
- [29] Scott M Lundberg et al. “From local explanations to global understanding with explainable AI for trees”. In: *Nature machine intelligence* 2.1 (2020), pp. 56–67.
- [30] Yining Ma, Zhiguang Cao, and Yeow Meng Chee. “Learning to Search Feasible and Infeasible Regions of Routing Problems with Flexible Neural k-Opt”. In: *Advances in Neural Information Processing Systems*. 2023.
- [31] Juan Pablo Mesa et al. “Machine-learning component for multi-start metaheuristics to solve the capacitated vehicle routing problem”. In: *Applied Soft Computing* 173 (2025), p. 112916. ISSN: 1568-4946.
- [32] Mouad Morabit, Guy Desaulniers, and Andrea Lodi. “Machine-learning-based column selection for column generation”. In: *Transportation Science* 55.4 (2021), pp. 815–831.
- [33] Mouad Morabit, Guy Desaulniers, and Andrea Lodi. “Learning to repeatedly solve routing problems”. In: *Networks* (2023).
- [34] Harikrishna Narasimhan, Rohit Vaish, and Shivani Agarwal. “On the statistical consistency of plug-in classifiers for non-decomposable performance measures”. In: *Advances in neural information processing systems* 27 (2014).
- [35] Caroline Prodhon and Christian Prins. “Metaheuristics for Vehicle Routing Problems”. In: *Metaheuristics*. Cham: Springer International Publishing, 2016, pp. 407–437.

- [36] Eduardo Queiroga et al. “10,000 optimal CVRP solutions for testing machine learning based heuristics”. In: *AAAI-22 Workshop on Machine Learning for Operations Research (ML4OR)* (2021).
- [37] J. Ross Quinlan. “Induction of decision trees”. In: *Machine learning* 1 (1986), pp. 81–106.
- [38] Ítalo Santana, Andrea Lodi, and Thibaut Vidal. “Neural Networks for Local Search and Crossover in Vehicle Routing: A Possible Overkill?” In: *International Conference on Integration of Constraint Programming, Artificial Intelligence, and Operations Research*. Springer. 2023, pp. 184–199.
- [39] Marina Sokolova and Guy Lapalme. “A systematic analysis of performance measures for classification tasks”. In: *Information processing & management* 45.4 (2009), pp. 427–437.
- [40] María Soto et al. “Multiple neighborhood search, tabu search and ejection chains for the multi-depot open vehicle routing problem”. In: *Computers & Industrial Engineering* 107 (2017), pp. 211–222.
- [41] Liang Xin et al. “NeuroLKH: Combining deep learning model with lin-kernighan-helsgaun heuristic for solving the traveling salesman problem”. In: *Advances in Neural Information Processing Systems* 34 (2021), pp. 7472–7483.
- [42] Artjom Zern, Klaus Broelemann, and Gjergji Kasneci. “Interventional shap values and interaction values for piecewise linear regression trees”. In: *Proceedings of the AAAI Conference on Artificial Intelligence*. 2023, pp. 11164–11173.